

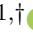
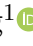




Original Research

METTL3/YTHDF1 Stabilizes MTCH2 mRNA to Regulate Ferroptosis in Glioma Cells

Hongjun Liu^{1,†}, Shasha Tan^{1,†}, Zhenyu Zhao^{1,†}, Xiaoping Tang¹, Zhou Li²,
Jian Qi^{1,*}

¹Department of Neurosurgery, The Affiliated Hospital of North Sichuan Medical College, 637000 Nanchong, Sichuan, China

²Department of Neurosurgery, The Affiliated Nanchong Central Hospital of North Sichuan Medical College, 637000 Nanchong, Sichuan, China

*Correspondence: 381010585@qq.com (Jian Qi)

†These authors contributed equally.

Academic Editor: Seok-Geun Lee

Submitted: 16 July 2024 Revised: 8 December 2024 Accepted: 12 December 2024 Published: 14 February 2025

Abstract

Background: Gliomas are aggressive brain tumors known for their poor prognosis and resistance to standard treatment options. Ferroptosis is an iron-dependent form of regulated cell death that has emerged as a promising target for cancer treatment. This study examined how the methyltransferase-like 3/YTH domain family protein 1 (*METTL3/YTHDF1*) axis influences ferroptosis and glioma progression by stabilizing mitochondrial carrier homolog 2 (*MTCH2*) messenger RNA (mRNA). **Methods:** *MTCH2* expression in glioma tissues and cell lines was evaluated through quantitative real-time polymerase chain reaction (PCR) and western blot analyses. To assess the effects of *MTCH2* knockdown and overexpression on glioma cell functions, we performed a series of functional assays, including cell viability, colony formation, and measurements of lipid reactive oxygen species (lipid ROS) and malondialdehyde (MDA) levels. Additionally, we conducted RNA immunoprecipitation (RIP) and RNA stability assays to explore the underlying mechanisms governing the interaction between *METTL3*, *YTHDF1*, and the stability of *MTCH2* mRNA. **Results:** *MTCH2* was significantly upregulated in glioma tissues and cell lines. Silencing of *MTCH2* resulted in decreased glioma cell proliferation and induced ferroptosis, as evidenced by increased lipid peroxidation and ROS accumulation. Conversely, overexpression of *MTCH2* enhanced glioma cell survival and reduced ferroptosis. *METTL3*-mediated N6-methyladenosine (m6A) modification enhanced *MTCH2* mRNA stability by enabling YTHDF1 to bind and protect the modified mRNA from degradation. **Conclusion:** The *METTL3/YTHDF1/MTCH2* axis plays a critical role in glioma progression by inhibiting ferroptosis and promoting tumor cell survival. Targeting this pathway may provide a new and effective treatment strategy for glioma patients.

Keywords: ferroptosis; m6A RNA methylation; glioma

1. Introduction

Glioma (GBM) is a highly aggressive and prevalent central nervous system tumor, predominantly affecting middle-aged and elderly individuals [1,2]. Symptoms such as headaches, seizures, and neurological deficits often lead to delayed diagnosis. Accounting for roughly 80% of brain tumors, gliomas have the highest mortality rate among central nervous system cancers [3]. The overall five-year survival rate for glioma patients is around 10–15%, but is significantly lower for advanced stages [4]. Prognosis depends on factors like diagnostic stage, age, and tumor molecular features [5,6]. Despite the availability of surgery, radiotherapy, and chemotherapy, recurrence and resistance remain major challenges, underscoring the need for innovative therapies [7,8].

Ferroptosis is a form of iron-dependent cell death characterized by the accumulation of lipid peroxides [9], has garnered substantial interest in cancer research, particularly in gliomas [10–12]. This pathway differs from traditional cell death processes like apoptosis, autophagy, and necrosis [13,14]. Its identification has opened new pos-

sibilities for effective cancer treatments [15]. It has been established that ferroptosis has a significant impact in various tumor types such as breast cancer [16], liver cancer [17], and glioma [18]. Core regulators, such as glutathione peroxidase 4 (*GPX4*) [19], solute carrier family 7 member 11 (*SLC7A11*) [20], and iron metabolism-related proteins, play critical roles in tumor initiation and progression. Current evidence shows that the growth and migration of glioma cells can be significantly inhibited by regulating key molecules in ferroptosis. Current studies reveal that modulating ferroptosis-related molecules inhibits glioma cell growth and migration. For instance, *GPX4* inhibition or increasing intracellular iron induces ferroptosis, hindering tumor growth [21,22]. Nevertheless, more research is required to comprehensively understand its role in gliomas.

MTCH2, a protein located in the outer mitochondrial membrane, is crucial for regulating lipid transport, energy metabolism, and apoptosis [23]. Previous research has linked *MTCH2* to the malignancy and prognosis of breast [24] and colorectal cancer [25], indicating its potential as a therapeutic target. Qiuyun Yuan *et al.* [26] demonstrated



that *MTCH2* expression correlates with GBM malignancy and resistance to temozolomide, underscoring its significance in GBM progression. Given the limited knowledge of *MTCH2*'s role in GBM and the critical involvement of mitochondria in ferroptosis [27], exploring the connection between *MTCH2* and ferroptosis in gliomas is crucial.

In the present study, *MTCH2* was found to be highly expressed in glioma tissues, and its expression was regulated through *METTL3* and *YTHDF1*-mediated N6-methyladenosine (m6A) methylation modification processes. Additionally, *MTCH2* was shown to regulate ferroptosis in glioma cells. Knockdown of *MTCH2* inhibited the malignant behavior of glioma cells. Therefore, it is suggested that *MTCH2* depletion may be a promising strategy to improve the prognosis of glioma.

2. Methods and Materials

2.1 Patient Samples

Between 2010 and 2024, 30 glioma tissue samples, along with their respective normal tissue counterparts, were obtained from the Affiliated Hospital of North Sichuan Medical College. Additionally, from 2022 to 2024, six matched pairs of glioma tissues and adjacent normal tissues were collected from the same institution specifically for Western blot analysis.

2.2 Culturing and Transfection of Cells

The GBM cell lines LN229 (CRL-2611, ATCC, Manassas, VA, USA), T98G (CRL-1690, ATCC, Manassas, VA, USA), and U251 (STCC11007G, Zixin Bio, Wuhan, Hubei, China), along with NHA (CP-H122, Pricella, Wuhan, Hubei, China), were maintained in Dulbecco's Modified Eagle Medium (DMEM; Gibco, Thermo Fisher Scientific, Waltham, MA, USA) supplemented with 10% fetal bovine serum (FBS; Gibco, Thermo Fisher Scientific, Waltham, MA, USA) and 1% penicillin/streptomycin (Sigma-Aldrich, St. Louis, MO, USA). Meanwhile, U87-MG cells (HTB-14, ATCC, Manassas, VA, USA) were cultured in complete Minimum Essential Medium (MEM; Gibco, Thermo Fisher Scientific, Waltham, MA, USA). Lentiviral vectors targeting the knockdown or overexpression of *MTCH2*, *WTAP*, *METTL3*, *METTL14*, and *YTHDF1*, as well as a control vector, were generated by GenePharma (Shanghai, China). GBM cells were cultured to approximately 70% confluence before plating in well plates and subsequently infected with the lentiviruses. Stable transfectants were obtained by selection with puromycin (4 µg/mL; Sigma-Aldrich, St. Louis, MO, USA) for two weeks. All cell lines were authenticated by short tandem repeat (STR) profiling and confirmed to be free of mycoplasma contamination.

2.3 Western Blotting

Western blot analysis was performed according to the method used in our previous publications [28]. All anti-

bodies used are listed in **Supplementary Table 1**. After incubation with the appropriate secondary antibodies, the membranes were developed using an enhanced chemiluminescence (ECL) detection reagent (ECL Plus Western Blotting Detection System, Cytiva, Marlborough, MA, USA) and analyzed using ImageJ software (version 1.54m, National Institutes of Health, Bethesda, MD, USA).

2.4 qRT-PCR

Total RNA was extracted from cells and tissues using the TRIzol reagent (Invitrogen, Thermo Fisher Scientific, Waltham, MA, USA) according to the manufacturer's instructions. Complementary DNA (cDNA) synthesis was performed using the One-Step RT-PCR Kit (Beyotime, Shanghai, China) following the manufacturer's protocols. Gene expression levels were analyzed using the BeyoFast™ SYBR Green One-Step RT-qPCR Kit (Beyotime, Shanghai, China) on a real-time PCR platform (Thermo Fisher Scientific, Waltham, MA, USA). The quantitative polymerase chain reaction (qPCR) procedure included reverse transcription at 50 °C for 15 minutes, an initial denaturation step at 95 °C for 5 minutes, followed by 40 cycles of amplification with denaturation at 95 °C for 10 seconds and annealing/extension at 60 °C for 30 seconds. Relative gene expression levels were calculated using the $2^{-\Delta\Delta C_t}$ method, with β -actin serving as the endogenous normalization control. The primer sequences used in these assays are listed in **Supplementary Table 2**.

2.5 Cell Proliferation

Transfected cells were seeded into 96-well plates, and the Cell Counting Kit-8 (CCK-8; Beyotime, Shanghai, China) reagent was added, followed by incubation at 37 °C for 1 hour. Absorbance was then measured at 450 nm using a microplate reader (BioTek, Winooski, VT, USA).

For the colony formation assay, approximately 500 cells were seeded per well in a 6-well plate (Corning, New York, USA) and cultured under standard conditions (37 °C with 5% CO₂) for 10–14 days. After washing with PBS (Gibco, Thermo Fisher Scientific, Waltham, MA, USA), cells were fixed with 4% paraformaldehyde (Beyotime, Shanghai, China) for 15 minutes and subsequently stained with 0.5% crystal violet (Sigma-Aldrich, St. Louis, MO, USA) for 15 minutes. Excess stain was removed by gentle rinsing, and the plates were air-dried before counting the colonies.

2.6 Ferroptosis Detection

Lipid reactive oxygen species (ROS) levels were evaluated using a 10 µM BODIPY-581/591 C11 probe (D3861, Thermo Fisher Scientific, Waltham, MA, USA). The treated cells were incubated with the probe for 30 minutes at 37 °C. After washing with PBS (Gibco, Thermo Fisher Scientific, Waltham, MA, USA), fluorescence intensity was measured using a microplate reader (BioTek, Winooski, VT, USA).

with excitation/emission wavelengths set at 488/510 nm for oxidized lipid ROS and 581/591 nm for reduced lipid ROS. The fluorescence data were analyzed to quantify lipid ROS levels.

Malondialdehyde (MDA) levels were assessed using the Lipid Peroxidation Assay Kit (ab118970, Abcam, Cambridge, UK). Lysates from cells or tissues were prepared and combined with the assay reagents according to the manufacturer's instructions. After incubation, absorbance at 532 nm was measured using a spectrophotometer (Thermo Fisher Scientific, Waltham, MA, USA) to evaluate lipid peroxidation levels.

2.7 Enzyme-Linked Immunosorbent Assay (ELISA)

The levels of 4-hydroxynonenal (4-HNE) in cell culture supernatants were quantified using a human 4-HNE ELISA kit (FineTest, Wuhan, Hubei, China), according to the manufacturer's instructions. Cell culture supernatants were collected by centrifugation at 3000 rpm for 10 minutes to remove debris. A standard curve was generated from serial dilutions of the provided 4-HNE standards. Both samples and standards were added to 96-well plates pre-coated with anti-4-HNE antibodies (FineTest, Wuhan, Hubei, China) and incubated at room temperature for 1 hour with gentle shaking.

After incubation, the plates were washed five times with the supplied wash buffer (FineTest, Wuhan, Hubei, China) to remove unbound substances. Horseradish peroxidase (HRP)-conjugated secondary antibodies (FineTest, Wuhan, Hubei, China) were then added to each well, and the plates were incubated at room temperature for 45 minutes. Following this incubation, the plates were washed an additional five times to remove excess antibodies.

TMB (3,3',5,5'-Tetramethylbenzidine) substrate (Thermo Fisher Scientific, Waltham, MA, USA) was added to each well for color development, and the plates were incubated in the dark at room temperature for 15 minutes. The reaction was stopped by adding 50 μ L of stop solution (Thermo Fisher Scientific, Waltham, MA, USA) per well, causing a color change from blue to yellow. Absorbance was measured at 450 nm using a microplate reader (BioTek, Winooski, VT, USA) within 10 minutes of adding the stop solution.

The concentrations of 4-HNE were determined by referencing the standard curve generated during the experiment.

2.8 RIP-qPCR Assay

For the RNA immunoprecipitation followed by quantitative polymerase chain reaction (RIP-qPCR) assay, cells were grown to approximately 70% confluence and lysed using RIP lysis buffer (Millipore, Burlington, MA, USA) supplemented with protease and RNase inhibitors (Sigma-Aldrich, St. Louis, MO, USA). The lysate was incubated at 4 °C for 4 hours with magnetic beads (Invitrogen, Thermo

Fisher Scientific, Waltham, MA, USA) conjugated to a specific antibody (1–5 μ g). After washing with RIP wash buffer (Millipore, Burlington, MA, USA), RNA-protein complexes were eluted using the elution buffer provided in the RIP kit (Magna, Millipore, Burlington, MA, USA). RNA was then extracted using the RNeasy Mini Kit (Qiagen, Hilden, Germany). The extracted RNA was reverse-transcribed into complementary DNA (cDNA) using a reverse transcription kit (Thermo Fisher Scientific, Waltham, MA, USA). qPCR with specific primers was subsequently performed to quantify the RNA targets associated with the immunoprecipitated proteins. All antibodies used are listed in **Supplementary Table 1**.

2.9 RNA Stability Assays

For the RNA stability assays, cells were grown to approximately 70% confluence and treated with 5 μ g/mL actinomycin D (Sigma-Aldrich, St. Louis, MO, USA) to inhibit transcription. Cells were then harvested at specified intervals (0, 2, 4, 6, and 8 hours), and total RNA was extracted using the RNeasy Mini Kit (Qiagen, Hilden, Germany). The extracted RNA was reverse-transcribed into cDNA using a reverse transcription kit (Thermo Fisher Scientific, Waltham, MA, USA), and qPCR with specific primers was performed to quantify the remaining RNA levels. The RNA half-life was calculated by fitting the RNA levels at different time points to an exponential decay model.

2.10 Cell Migration and Invasion Analysis

For the migration assay, cells were seeded into the upper chamber of a Transwell insert (Corning, New York, USA) with 10% FBS in the lower chamber. After 24 hours of incubation, cells on the upper surface were removed, and the migrated cells on the lower surface were fixed with 4% paraformaldehyde (Beyotime, Shanghai, China), stained with 0.5% crystal violet (Sigma-Aldrich, St. Louis, MO, USA), and counted.

For the invasion assay, the upper chamber was coated with Matrigel (Corning, New York, USA), and cells were incubated for 48 hours before analysis. The results were compared between *MTCH2* knockdown and overexpression groups to assess their effects on glioma cell invasion.

2.11 Statistical Analysis

Data were analyzed using GraphPad Prism (GraphPad Software, San Diego, CA, USA). Results are expressed as the mean \pm standard deviation (SD), with details on sample size and replication provided in the figure legends. Comparisons between groups were performed using either Student's *t*-test or ANOVA, as appropriate. A *p*-value of less than 0.05 was considered statistically significant.

3. Results

3.1 *MTCH2* Expression is Increased in GBM and Drives Growth

To investigate the function of *MTCH2* in glioma, we began by examining its expression levels in glioma tissue samples. *MTCH2* messenger RNA (mRNA) levels were increased in an internal cohort of glioma tissues, as determined by qPCR (Fig. 1A). Western blot analysis of tissue samples further confirmed significantly increased mitochondrial carrier homolog 2 (*MTCH2*) protein levels in glioma compared to normal tissue (Fig. 1B,C). The involvement of *MTCH2* in glioma growth was examined *in vitro* using five different cell lines, including LN229, U87MG, U251, and T98G. The findings revealed that *MTCH2* expression was notably higher in LN229 and U87MG cells, while it was comparatively lower in T98G cells (Fig. 1D). *MTCH2* expression was regulated in LN229 and U87MG cell lines by short hairpin RNA (shRNA) knockdown and overexpression systems, respectively (Fig. 1E,F). The CCK-8 assay revealed that knockdown of *MTCH2* expression reduced glioma cell viability, whereas overexpression of *MTCH2* significantly increased viability (Fig. 2A,B). Furthermore, colony formation assays revealed that *MTCH2*-deficient glioma cells formed fewer colonies, whereas *MTCH2*-overexpressing cells formed more colonies (Fig. 2C,D). Transwell assays demonstrated that *MTCH2* knockdown reduced glioma cell migration and invasion, whereas *MTCH2* overexpression significantly enhanced both migration and invasion capabilities (Fig. 2E,F). In addition, we selected T98G cells with lower *MTCH2* expression for overexpression experiments (Supplementary Fig. 1A,B). The CCK-8 assay demonstrated that overexpression of *MTCH2* notably enhanced the proliferation of T98G cells. Subsequently, the colony formation assay further demonstrated that cells overexpressing *MTCH2* formed more colonies, confirming the role of *MTCH2* in promoting cell proliferation (Supplementary Fig. 1C,D). Additionally, the Transwell migration and invasion assays indicated that *MTCH2* overexpression markedly promoted the migratory and invasive capabilities of T98G cells (Supplementary Fig. 1E). These findings further confirm the crucial role of *MTCH2* in promoting glioma cell proliferation, migration, and invasion. Overall, these results demonstrate that *MTCH2* is strongly upregulated in GBM and contributes toward glioma cell survival and proliferation.

3.2 *MTCH2* Regulates Glioma Growth through Ferroptosis

MTCH2 generally inhibits ferroptosis, and depletion of *MTCH2* in glioma cells led to increased 4-HNE production, higher levels of lipid ROS and MDA, and decreased GPX4 protein expression (Fig. 3A–D). In contrast, the overexpression of *MTCH2* reversed these phenomena (Fig. 3E,F). In addition, Ferrostatin-1 partially restores the

colony formation ability impaired by *MTCH2* knockdown, further demonstrating that *MTCH2* regulates glioma cell proliferation by modulating ferroptosis (Supplementary Fig. 2A,B). To further elucidate the role of *MTCH2* in ferroptosis, Western blot analysis was performed on the glioma cell lines LN229 and U87MG. As shown in Fig. 3G, *MTCH2* knockdown significantly increased the expression of transferrin receptor (TFRC) and NADPH oxidase 4 (NOX4), which are involved in iron metabolism and oxidative stress, respectively. Conversely, transferrin (TF) levels were notably elevated, whereas ferritin light chain (FLT) levels showed a significant decrease. In contrast, overexpression of *MTCH2* led to decreased expression of TFRC and NOX4, but increased levels of TF and FLT. These findings indicate that *MTCH2* is critical in the regulation of ferroptosis and could thus affect the growth and development of gliomas.

3.3 *METTL3* Promotes *MTCH2* Expression by Facilitating m6A Modification

The sequence-based RNA adenosine methyltransferase site predictor (SRAMP) identified multiple m6A sites within the *MTCH2* mRNA sequence (Fig. 4A). The m6A RNA immunoprecipitation assay was used to quantify *MTCH2* mRNA m6A levels in NHA cells and glioma cell lines. This revealed significant enrichment by m6A-specific antibodies in both cell types. Of note, glioma cell lines exhibited higher levels of m6A-modified *MTCH2* mRNA compared to NHA cells (Fig. 4B).

To explore the m6A modification mechanism of *MTCH2* mRNA, we analyzed the three primary components of the methyltransferase complex: *WTAP*, *METTL3*, and *METTL14*. Next, qPCR analysis was performed on glioma and normal tissue samples. The results showed that *METTL3* mRNA levels were significantly elevated in glioma tissues, while no significant differences were observed for *METTL14* and *WTAP* mRNA levels (Supplementary Fig. 3A–C). Western blot analysis further confirmed that *METTL3* protein expression was higher in glioma tissues compared to matched normal tissues (Supplementary Fig. 3D), supporting the role of *METTL3* in glioma progression. Knockdown of *WTAP*, *METTL3*, and *METTL14* significantly reduced *MTCH2* mRNA levels in glioma cells, with depletion of *METTL3* having the most notable effect (Supplementary Fig. 3E, Fig. 4C). Conversely, the overexpression of *WTAP*, *METTL3*, and *METTL14* increased *MTCH2* mRNA levels, particularly with *METTL3* (Supplementary Fig. 3F, Fig. 4D). Therefore, *METTL3* appears to play a crucial role in the post-transcriptional modification of *MTCH2*.

Knockdown of *METTL3* in glioma cells led to decreased *METTL3* mRNA and *MTCH2* protein levels, as well as decreased *MTCH2* mRNA and *MTCH2* protein levels (Fig. 4E–H), whereas *METTL3* overexpression led to higher levels of both *METTL3* and *MTCH2* proteins

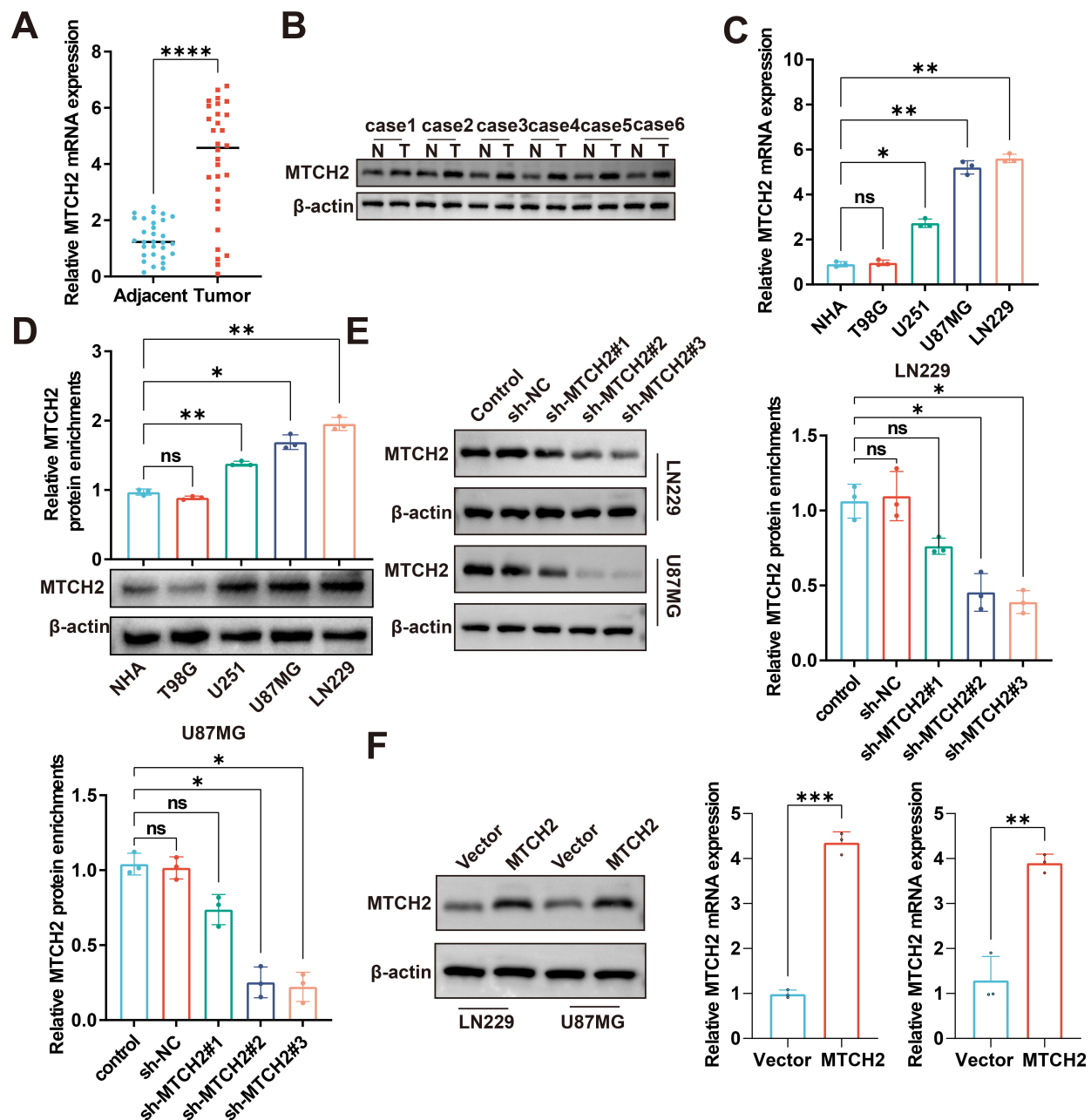


Fig. 1. *MTCH2* expression is upregulated in GBM. (A) *MTCH2* mRNA levels in 30 cases of glioma and adjacent normal tissues from an internal cohort, measured using qRT-PCR. (B) *MTCH2* protein levels in six pairs of fresh glioma and adjacent normal tissues from an internal cohort, detected by Western blotting. (C,D) *MTCH2* mRNA (C) and *MTCH2* protein (D) levels were analyzed in glioma and normal cell lines using qRT-PCR and Western blot, respectively. (E,F) *MTCH2* protein levels were analyzed in glioma cells following *MTCH2* knockdown (E) and *MTCH2* overexpression (F). ns, not significant, * $p < 0.05$, ** $p < 0.01$, *** $p < 0.001$, **** $p < 0.0001$. qRT-PCR, quantitative reverse transcription polymerase chain reaction; mRNA, messenger RNA; *MTCH2*, mitochondrial carrier homolog 2; sh-NC, short hairpin RNA negative control; sh-*MTCH2*#1, short hairpin RNA targeting *MTCH2*, clone #1.

(Fig. 4I,J). Immunoprecipitation of METTL3 from cytoplasmic extracts of glioma cells revealed significant enrichment of *MTCH2* mRNA compared to the IgG control (Fig. 4K), indicating an interaction between METTL3 and *MTCH2* mRNA. Overexpression of *METTL3* increased this enrichment, whereas *METTL3* silencing reduced it (Fig. 4L,M).

To determine if *MTCH2* regulation is m6A-dependent, a RIP assay was performed using an m6A-specific antibody. Disruption of *METTL3* decreased m6A-modified *MTCH2* mRNA, whereas *METTL3* overexpression increased it. An RNA stability assay showed that *METTL3* depletion shortened the *MTCH2* mRNA half-life, whereas *METTL3* overexpression prolonged it, suggesting that m6A

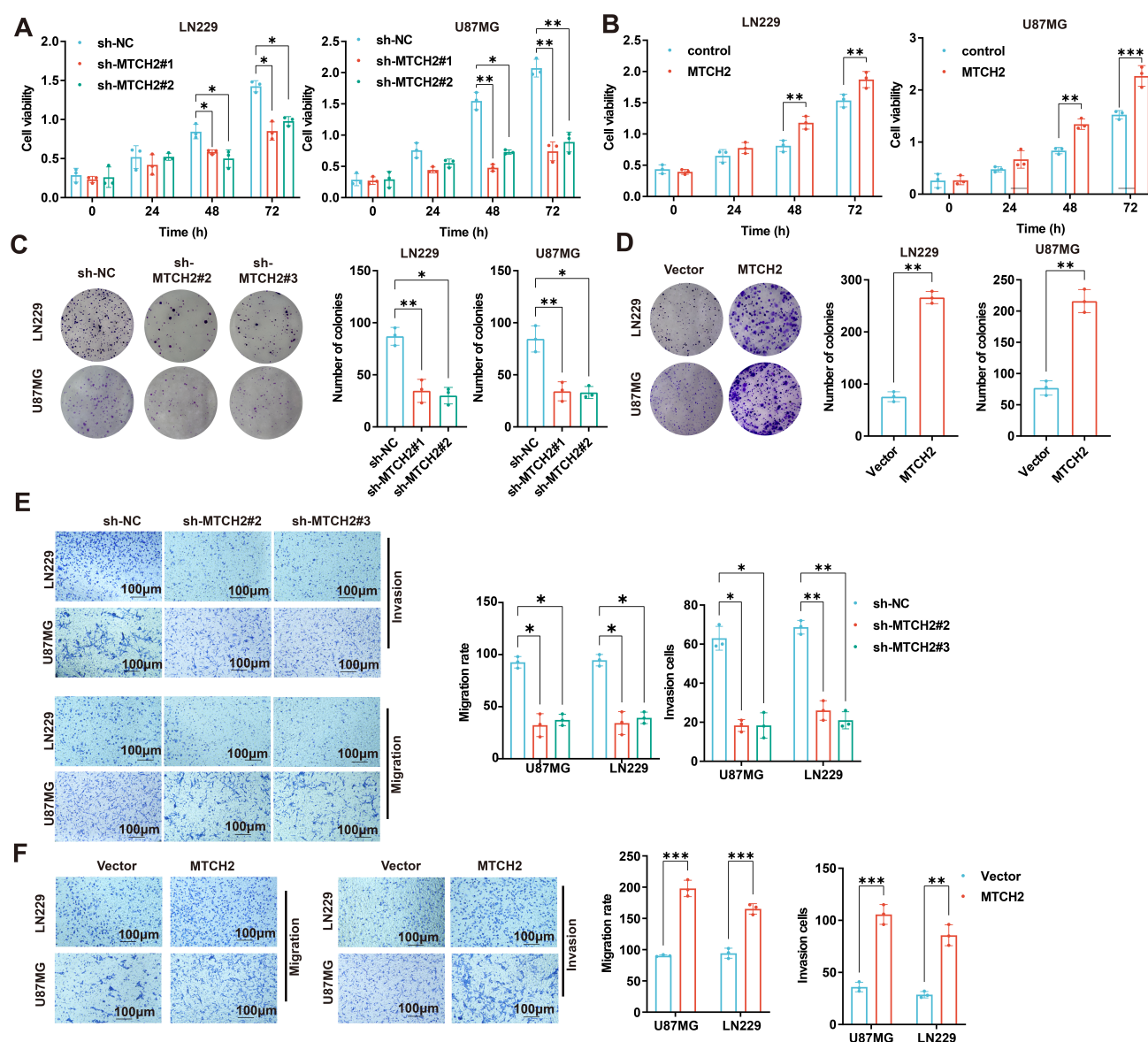


Fig. 2. The effect of *MTCH2* on glioma cells. (A,B) The viability of glioma cells, including various glioma cell lines, following *MTCH2* knockdown (A) or *MTCH2* overexpression (B), was assessed using the CCK-8 assay. (C,D) Colony formation ability of glioma cells following *MTCH2* knockdown (C) and *MTCH2* overexpression (D) was evaluated. (E,F) Transwell migration and invasion assays of glioma cells were performed to evaluate the effects of *MTCH2* knockdown (E) and *MTCH2* overexpression (F). Scale bar: 100 μ m. * p < 0.05, ** p < 0.01, *** p < 0.001. CCK-8, Cell Counting Kit-8.

modification stabilizes *MTCH2* mRNA (Fig. 4N,O). These findings indicate that *METTL3*-induced m6A modification enhances the expression of *MTCH2* by stabilizing its mRNA.

3.4 *YTHDF1* Safeguards *MTCH2* mRNA that has Undergone m6A Modification

The mechanism through which m6A modification contributes to the stabilization of *MTCH2* mRNA involves *YTHDF1*. This well-known m6A reader protein plays a role in the nuclear export, translation, and stability of target RNAs. Elevated *YTHDF1* mRNA levels were also ob-

served in the internal cohort (Fig. 5A). *MTCH2* mRNA in glioma cells showed a significantly stronger association with YTH domain family protein 1 (*YTHDF1*) compared to the IgG control (Fig. 5B). Knockdown of *YTHDF1* resulted in decreased *YTHDF1* and *MTCH2* mRNA levels (Fig. 5C,D), whereas overexpression of *YTHDF1* led to increased *YTHDF1* and *MTCH2* mRNA levels (Fig. 5E). At the protein level, knockdown of *YTHDF1* reduced the protein levels of both *YTHDF1* and *MTCH2*, while overexpression of *YTHDF1* significantly increased their protein levels (Fig. 5F,G). Additionally, knockdown of *YTHDF1* reduced the interaction between *MTCH2* mRNA

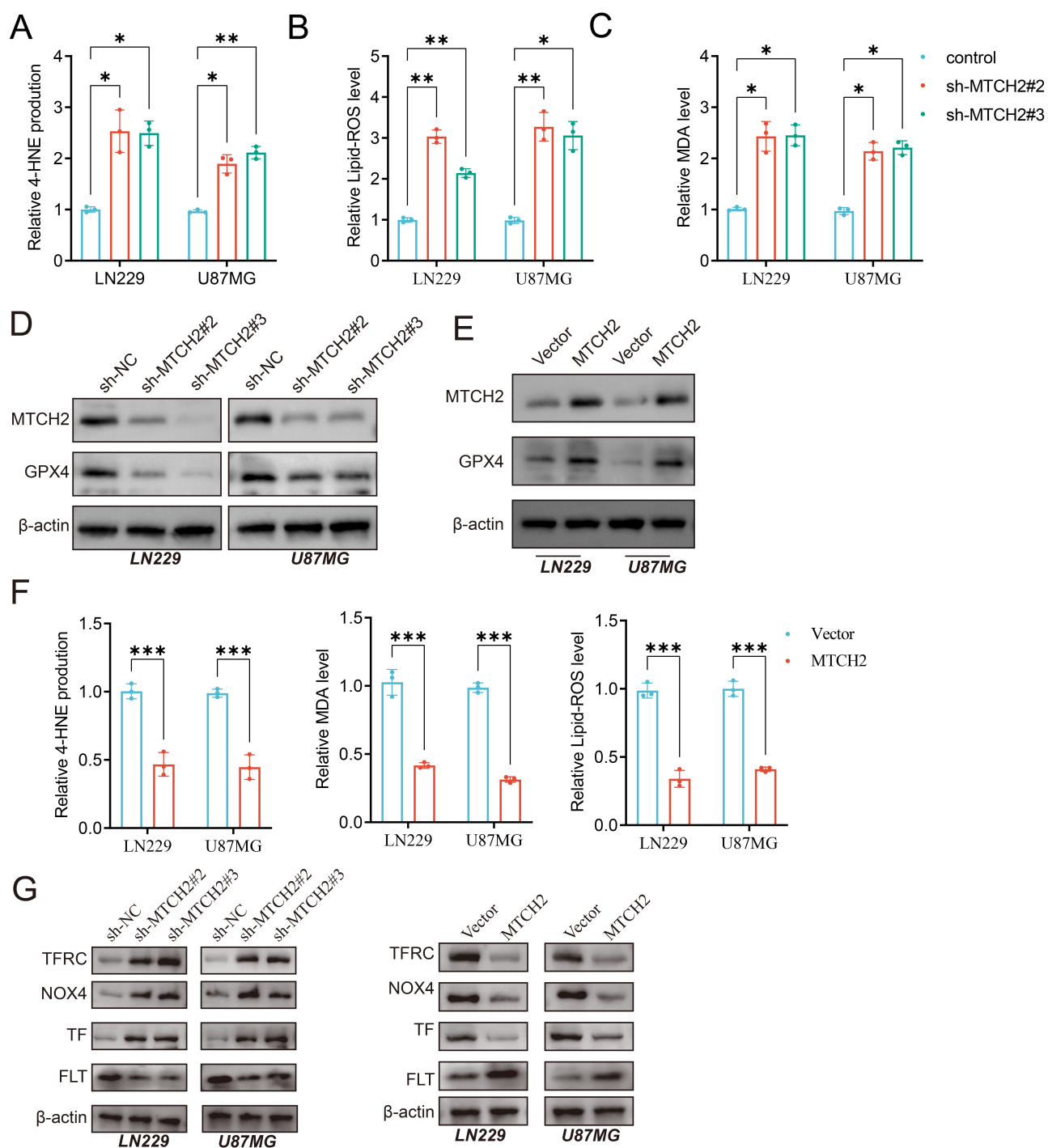


Fig. 3. *MTCH2* promotes the progression of gliomas by inhibiting ferroptosis. (A–C) The levels of 4-HNE, lipid ROS, and MDA in glioma cells with *MTCH2* depletion ($n = 3$). (D) Levels of GPX4 protein in glioma cells with *MTCH2* depletion ($n = 3$). (E) Levels of GPX4 protein in glioma cells with *MTCH2* overexpression ($n = 3$). (F) Levels of 4-HNE, lipid ROS, and MDA in glioma cells with *MTCH2* overexpression ($n = 3$). (G) Western blot analysis showing the effects of *MTCH2* knockdown or overexpression on TFRC, NOX4, TF, and FLT expression levels in glioma cells. * $p < 0.05$, ** $p < 0.01$, *** $p < 0.001$. MDA, malondialdehyde; ROS, reactive oxygen species; 4-HNE, 4-hydroxynonenal; TFRC, transferrin receptor; NOX4, NADPH oxidase 4; TF, transferrin; GPX4, glutathione peroxidase 4; FLT, ferritin light chain.

and YTHDF1 (Fig. 5H,I). RNA stability assays demonstrated that knockdown of *YTHDF1* shortened the half-life of *MTCH2* mRNA (Fig. 5J). These results suggest that

YTHDF1 promotes the expression of *MTCH2* in glioma cells by enhancing the stability of m6A-modified *MTCH2* mRNA. At the same time, through clone formation experi-

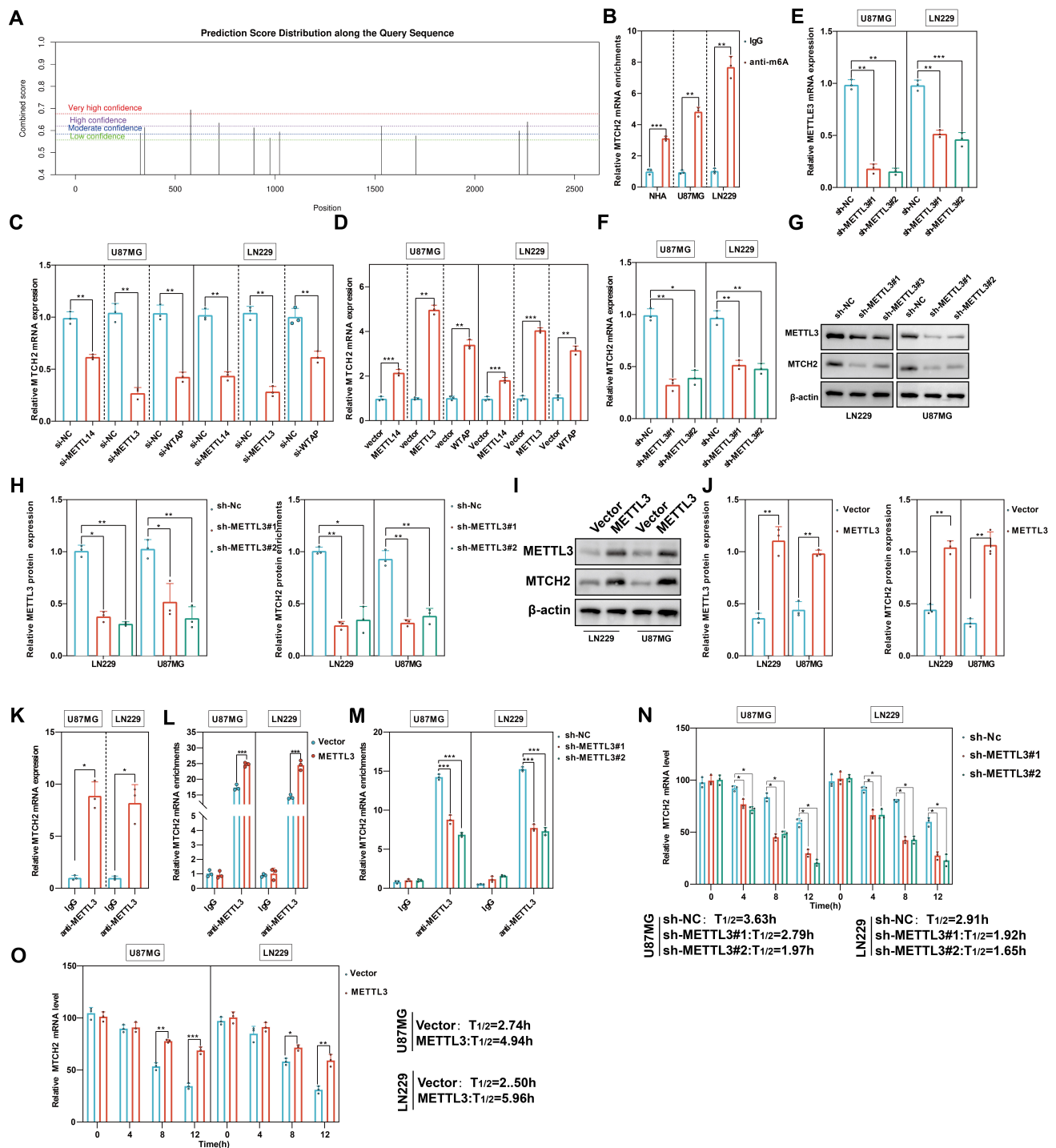


Fig. 4. METTL3 facilitates the upregulation of MTCH2 by increasing its m6A modification levels. (A) Predicted sites for m6A modifications in the MTCH2 mRNA sequence. (B) Levels of m6A modification in NHA and GBM cell lines were analyzed using an m6A-RIP assay (n = 3). (C,D) The expression levels of MTCH2 mRNA were quantified in GBM cells following knockdown or overexpression of METTL14, METTL3, and WTAP (n = 3). (E–H) Evaluation of METTL3 and MTCH2 mRNA and their corresponding protein levels after METTL3 knockdown in GBM cells (n = 3). (I,J) Analysis of changes in METTL3 and MTCH2 protein levels due to METTL3 overexpression in GBM cells (n = 3). (K) METTL3-bound MTCH2 mRNA is significantly enriched in glioma cells. (L,M) Assessment of how METTL3 overexpression or silencing impacts its binding affinity to MTCH2 mRNA (n = 3). (N,O) In GBM cells, MTCH2 mRNA exhibited accelerated degradation upon METTL3 knockdown, whereas METTL3 overexpression led to a slower degradation rate (n = 3). Transcription was inhibited using actinomycin D (AcTD) at 5 µg/mL for specified time points, and MTCH2 mRNA levels were quantified by RT-qPCR. * $p < 0.05$, ** $p < 0.01$, *** $p < 0.001$. m6A, N6-methyladenosine; RIP, RNA immunoprecipitation; METTL3, methyltransferase-like 3.

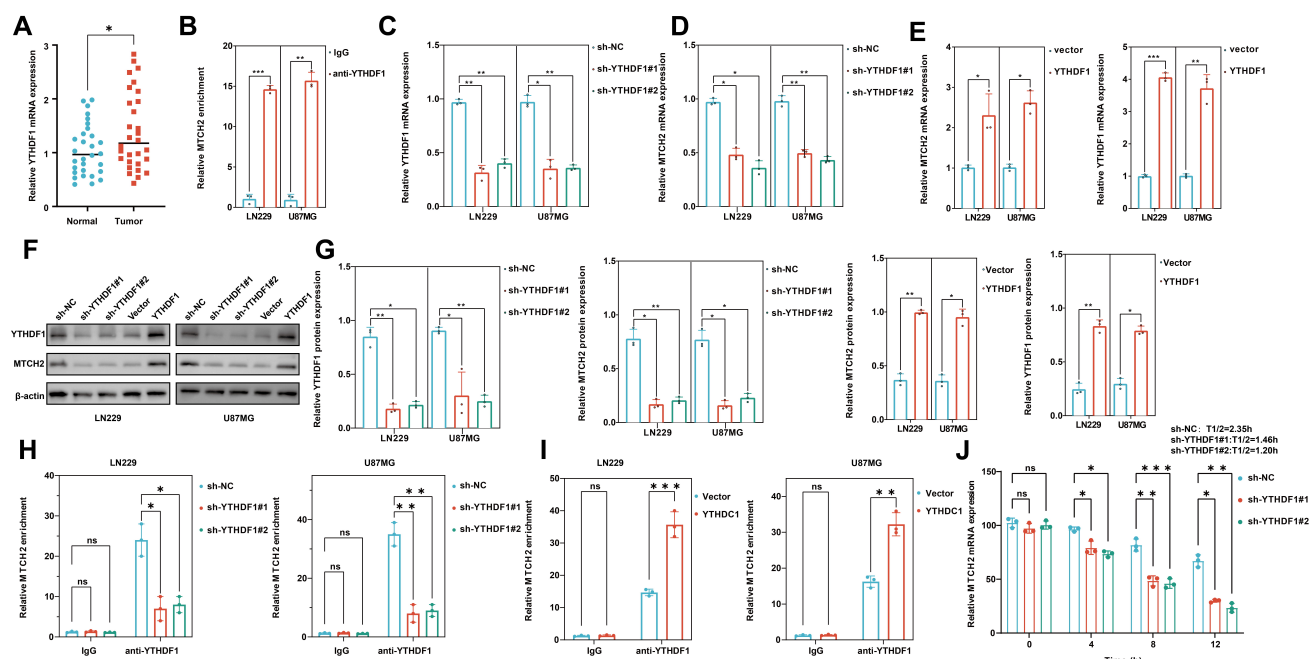


Fig. 5. *YTHDF1* increased the stability of *MTCH2*. (A) Expression of *YTHDF1* mRNA in gliomas from the internal cohort. (B) Verification of *YTHDF1* binding to *MTCH2* mRNA in GBM cells via RIP assay. (C–E) *YTHDF1* and *MTCH2* mRNA levels in GBM cells with *YTHDF1* knockdown or overexpression ($n = 3$). (F,G) *YTHDF1* and *MTCH2* protein levels in GBM cells with *YTHDF1* knockdown or overexpression ($n = 3$). (H) Effect of *YTHDF1* knockdown on the binding of YTH domain family protein 1 (*YTHDF1*) to *MTCH2* mRNA in GBM cells. (I) Effect of *YTHDF1* overexpression on the binding of *YTHDF1* to *MTCH2* mRNA in GBM cells. (J) Rapid degradation of *MTCH2* mRNA in GBM cells with *YTHDF1* knockdown. ns, not significant, $*p < 0.05$, $**p < 0.01$, $***p < 0.001$. *YTHDF1*, YTH domain family protein 1.

ments, we also found that *METTL3* and *YTHDF1* modulate the growth of GBM cells by upregulating the expression of *MTCH2* (Supplementary Fig. 4).

3.5 *METTL3/YTHDF1* Modulates Ferroptosis through the Upregulation of *MTCH2* Expression

The mechanism through which m6A modification contributes to the stabilization of *MTCH2* mRNA involves *YTHDF1*. To further validate whether *METTL3* and *YTHDF1* influence ferroptosis in GBM by enhancing *MTCH2* expression, we reintroduced *MTCH2* into *METTL3*- or *YTHDF1*-deficient GBM cells. Depletion of *METTL3* or *YTHDF1* resulted in reduced cell viability and increased levels of 4-HNE, lipid ROS, and MDA (Fig. 6A–D), indicating that their absence promotes ferroptosis. Notably, re-expressing *MTCH2* counteracted the ferroptosis enhancement observed upon *METTL3* or *YTHDF1* depletion. Additionally, we silenced *MTCH2* in GBM cells overexpressing *METTL3* or *YTHDF1*. *METTL3* or *YTHDF1* overexpression inhibited ferroptosis, whereas *MTCH2* knockdown reversed this ferroptosis suppression (Fig. 6E–H), suggesting that *METTL3* and *YTHDF1* regulate ferroptosis in GBM cells by modulating *MTCH2* expression. Overall, these findings provide evidence that *METTL3* and *YTHDF1* suppress ferroptosis by enhancing the expression of *MTCH2*.

4. Discussion

The primary clinical challenges in the treatment of glioma are its high heterogeneity and resistance to conventional therapies, leading to poor prognosis and a high recurrence rate [29]. Therefore, finding more effective therapeutic targets is of great significance in addressing this clinical problem. The present study elucidated a novel molecular mechanism involving the *METTL3-YTHDF1* axis that underlies the regulation of ferroptosis in gliomas. *METTL3* appears to play a pivotal role in promoting the growth of gliomas by stabilizing *MTCH2* mRNA through m6A modification, which is then recognized and bound by *YTHDF1*. This interaction subsequently enhances the regulation of ferroptosis.

The current findings highlight the significant contribution of the *METTL3*-m6A-*YTHDF1*-*MTCH2* pathway to metabolic reprogramming associated with regulation of ferroptosis in glioma cells and the fostering of a conducive environment for tumor progression. By delineating this pathway, the present study has increased our understanding of the molecular dynamics at play in glioma development, while identifying potentially novel therapeutic targets within this axis.

N6-methyladenosine (m6A) methylation is a prevalent and significant RNA modification found in eukaryotic

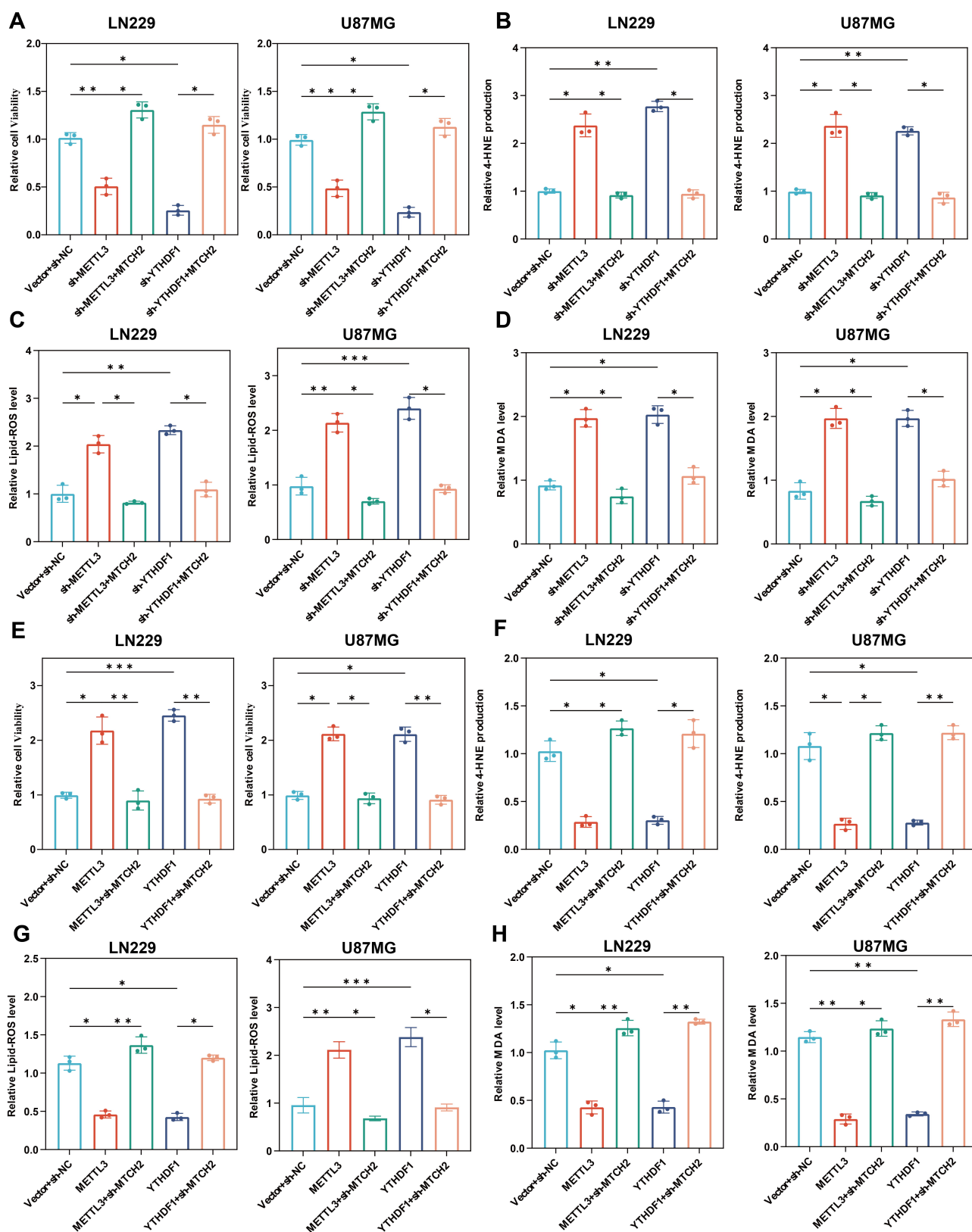


Fig. 6. *METTL3* and *YTHDF1* regulate ferroptosis in GBM cells by increasing the expression of *MTCH2*. (A,E) The viability of GBM cells was measured by a CCK-8 assay. (B,F) The level of 4-HNE in transfected GBM cells. (C,G) Lipid peroxidation levels in transfected GBM cells. (D,H) MDA levels in transfected GBM cells. * $p < 0.05$, ** $p < 0.01$, *** $p < 0.001$.

mRNA [30,31]. It plays a key role in the regulation of gene expression by affecting RNA stability, splicing, translation, and degradation [31]. m6A modification is carried out by a group of specialized enzymes, including “writer” enzymes (mainly the *METTL3/METTL14* complexes [32]), “reader” proteins (such as the *YTHDF* [33] and *YTHDC* families [34]), and “eraser” enzymes (such as *FTO* [35] and *ALKBH5* [36]). These enzymes regulate the fate and function of RNA by adding, recognizing, and removing m6A modifications [37].

Current evidence indicates that m6A methylation is crucial for maintaining the characteristics of tumor stem cells, and for mediating immune escape [38,39]. The present study found that *METTL3*-induced m6A modification enhanced the expression of *MTCH2*, and that *YTHDF1* maintained the stability of this expression. Moreover, these complex regulations ultimately lead to high expression levels of *MTCH2* in glioma.

Recent studies suggest that methylation processes significantly affect ferroptosis in tumor cells [40]. For example, the m6A ‘writer’ enzyme *METTL3* modifies several mRNAs associated with iron metabolism (e.g., *FTH1* [41] and *SLC7A11* [42]) to regulate their stability and translation efficiency, thereby influencing intracellular iron levels and lipid peroxidation. In addition, m6A methylation can directly impact the accumulation of lipid peroxides by regulating lipid metabolism genes, thus inducing or preventing ferroptosis in tumor cells [43]. There are currently very few published studies on the regulatory role of *MTCH2* in ferroptosis [44]. The present research findings therefore contribute to knowledge in this field. Nevertheless, further studies are essential to elucidate precise mechanism underlying *MTCH2*-mediated inhibition of ferroptosis.

It is important to consider the potential clinical applications associated with the *METTL3/YTHDF1/MTCH2* axis in the regulation of glioma. Since *METTL3* promotes *MTCH2* expression through m6A methylation and its mRNA is stabilized via *YTHDF1* recognition. Inhibiting the activity of *METTL3* or *YTHDF1* may disrupt the *MTCH2*-mediated regulation of ferroptosis, thereby reducing tumor cell survival and increasing the sensitivity of glioma to therapies. As the role of m6A methylation in cancer becomes increasingly clear, the development of drugs that target the m6A modification process (e.g., small molecule inhibitors, specific antibodies) could offer new therapeutic options for glioma patients [45]. The targeting of this axis may be effective as a standalone therapy. Alternatively, it could be integrated with existing treatments such as radiation, chemotherapy, or immunotherapy to create multi-targeted strategies that enhance therapeutic outcomes and improve patient survival. Therefore, further investigation into the *METTL3/YTHDF1/MTCH2* axis in glioma is important not only to gain a better understanding of its molecular mechanisms, but also for potential future clinical applications.

A limitation of this study is that the GBM cell lines were cultured under normoxic conditions (i.e., 37 °C with 5% CO₂). However, the actual tumor microenvironment (TME) often exhibits hypoxia. In future research, we intend to investigate the impact of *MTCH2* on GBM progression under hypoxic conditions in order to better mimic the *in vivo* TME. At the same time, more studies will be needed to delineate plausible link between *MTCH2* and other known ferroptosis pathways.

5. Conclusion

This study describes a complex regulatory axis (*METTL3*-m6A-*YTHDF1*-*MTCH2*-ferroptosis) in gliomas. Targeting this pathway could offer a promising strategy for developing more effective therapeutic interventions for patients with this complex malignancy.

Availability of Data and Materials

The data supporting the findings and the materials used in this study are available from the corresponding author upon reasonable request.

Author Contributions

HJL was responsible for conceptualization, methodology, writing the original draft, and supervision. SST, ZYZ, ZL and XPT contributed to data curation, investigation, and formal analysis. JQ handled visualization, software, and validation. In addition, ZL was in charge of resources, funding acquisition, and project administration. XPT managed writing, reviewing, editing, supervision, and project administration. All authors contributed to editorial changes in the manuscript. All authors have read and agreed to the published version of the manuscript. All authors have participated sufficiently in the work and agreed to be accountable for all aspects of the work.

Ethics Approval and Consent to Participate

The study was carried out in accordance with the guidelines of the Declaration of Helsinki. A written consent was signed by the patients or their families/legal guardians. This study received ethical approval from North Sichuan Medical College (Approval No. 2024059).

Acknowledgment

We sincerely thank the reviewers for their valuable feedback and suggestions, which have been instrumental in improving this manuscript.

Funding

This work was supported by Project of City-University Science and Technology Strategic Cooperation of Nanchong City (No. 22SXQT0035) and Project of City-University Science and Technology Strategic Cooperation of Nanchong City (No. 22SXQT0023).

Conflict of Interest

The authors declare no conflict of interest.

Supplementary Material

Supplementary material associated with this article can be found, in the online version, at <https://doi.org/10.31083/FBL25718>.

References

- [1] Weller M, Wick W, Aldape K, Brada M, Berger M, Pfister SM, *et al.* Glioma. *Nature Reviews. Disease Primers.* 2015; 1: 15017. <https://doi.org/10.1038/nrdp.2015.17>.
- [2] Ostrom QT, Bauchet L, Davis FG, Deltour I, Fisher JL, Langer CE, *et al.* The epidemiology of glioma in adults: a “state of the science” review. *Neuro-oncology.* 2014; 16: 896–913. <https://doi.org/10.1093/neuonc/nou087>.
- [3] Lapointe S, Perry A, Butowski NA. Primary brain tumours in adults. *Lancet (London, England).* 2018; 392: 432–446. [https://doi.org/10.1016/S0140-6736\(18\)30990-5](https://doi.org/10.1016/S0140-6736(18)30990-5).
- [4] Chen R, Smith-Cohn M, Cohen AL, Colman H. Glioma Subclassifications and Their Clinical Significance. *Neurotherapeutics: the Journal of the American Society for Experimental NeuroTherapeutics.* 2017; 14: 284–297. <https://doi.org/10.1007/s13311-017-0519-x>.
- [5] Barthel L, Hadamitzky M, Dammann P, Schedlowski M, Sure U, Thakur BK, *et al.* Glioma: molecular signature and crossroads with tumor microenvironment. *Cancer Metastasis Reviews.* 2022; 41: 53–75. <https://doi.org/10.1007/s10555-021-09997-9>.
- [6] Yang K, Wu Z, Zhang H, Zhang N, Wu W, Wang Z, *et al.* Glioma targeted therapy: insight into future of molecular approaches. *Molecular Cancer.* 2022; 21: 39. <https://doi.org/10.1186/s12943-022-01513-z>.
- [7] Xu S, Tang L, Li X, Fan F, Liu Z. Immunotherapy for glioma: Current management and future application. *Cancer Letters.* 2020; 476: 1–12. <https://doi.org/10.1016/j.canlet.2020.02.002>.
- [8] Nicholson JG, Fine HA. Diffuse Glioma Heterogeneity and Its Therapeutic Implications. *Cancer Discovery.* 2021; 11: 575–590. <https://doi.org/10.1158/2159-8290.CD-20-1474>.
- [9] Jiang X, Stockwell BR, Conrad M. Ferroptosis: mechanisms, biology and role in disease. *Nature Reviews. Molecular Cell Biology.* 2021; 22: 266–282. <https://doi.org/10.1038/s41580-020-00324-8>.
- [10] Li D, Li Y. The interaction between ferroptosis and lipid metabolism in cancer. *Signal Transduction and Targeted Therapy.* 2020; 5: 108. <https://doi.org/10.1038/s41392-020-00216-5>.
- [11] Liu T, Zhu C, Chen X, Guan G, Zou C, Shen S, *et al.* Ferroptosis, as the most enriched programmed cell death process in glioma, induces immunosuppression and immunotherapy resistance. *Neuro-Oncology.* 2022; 24: 1113–1125. <https://doi.org/10.1093/neuonc/noac033>.
- [12] Li K, Chen B, Xu A, Shen J, Li K, Hao K, *et al.* TRIM7 modulates NCOA4-mediated ferritinophagy and ferroptosis in glioblastoma cells. *Redox Biology.* 2022; 56: 102451. <https://doi.org/10.1016/j.redox.2022.102451>.
- [13] Mou Y, Wang J, Wu J, He D, Zhang C, Duan C, *et al.* Ferroptosis, a new form of cell death: opportunities and challenges in cancer. *Journal of Hematology & Oncology.* 2019; 12: 34. <https://doi.org/10.1186/s13045-019-0720-y>.
- [14] Tang D, Chen X, Kang R, Kroemer G. Ferroptosis: molecular mechanisms and health implications. *Cell Research.* 2021; 31: 107–125. <https://doi.org/10.1038/s41422-020-00441-1>.
- [15] Tong X, Tang R, Xiao M, Xu J, Wang W, Zhang B, *et al.* Targeting cell death pathways for cancer therapy: recent developments in necroptosis, pyroptosis, ferroptosis, and cuproptosis research. *Journal of Hematology & Oncology.* 2022; 15: 174. <https://doi.org/10.1186/s13045-022-01392-3>.
- [16] Li H, Yang P, Wang J, Zhang J, Ma Q, Jiang Y, *et al.* HLF regulates ferroptosis, development and chemoresistance of triple-negative breast cancer by activating tumor cell-macrophage crosstalk. *Journal of Hematology & Oncology.* 2022; 15: 2. <https://doi.org/10.1186/s13045-021-01223-x>.
- [17] Zheng C, Zhang B, Li Y, Liu K, Wei W, Liang S, *et al.* Donafenib and GSK-J4 Synergistically Induce Ferroptosis in Liver Cancer by Upregulating HMOX1 Expression. *Advanced Science.* 2023; 10: e2206798. <https://doi.org/10.1002/advs.202206798>.
- [18] Han L, Zhou J, Li L, Wu X, Shi Y, Cui W, *et al.* SLC1A5 enhances malignant phenotypes through modulating ferroptosis status and immune microenvironment in glioma. *Cell Death & Disease.* 2022; 13: 1071. <https://doi.org/10.1038/s41419-022-05526-w>.
- [19] Liang D, Feng Y, Zandkarimi F, Wang H, Zhang Z, Kim J, *et al.* Ferroptosis surveillance independent of GPX4 and differentially regulated by sex hormones. *Cell.* 2023; 186: 2748–2764.e22. <https://doi.org/10.1016/j.cell.2023.05.003>.
- [20] He F, Zhang P, Liu J, Wang R, Kaufman RJ, Yaden BC, *et al.* ATF4 suppresses hepatocarcinogenesis by inducing SLC7A11 (xCT) to block stress-related ferroptosis. *Journal of Hepatology.* 2023; 79: 362–377. <https://doi.org/10.1016/j.jhep.2023.03.016>.
- [21] Wang Z, Xia Y, Wang Y, Zhu R, Li H, Liu Y, *et al.* The E3 ligase TRIM26 suppresses ferroptosis through catalyzing K63-linked ubiquitination of GPX4 in glioma. *Cell Death & Disease.* 2023; 14: 695. <https://doi.org/10.1038/s41419-023-06222-z>.
- [22] Chen J, Li T, Zhou N, He Y, Zhong J, Ma C, *et al.* Engineered Salmonella inhibits GPX4 expression and induces ferroptosis to suppress glioma growth in vitro and in vivo. *Journal of Neuro-oncology.* 2023; 163: 607–622. <https://doi.org/10.1007/s11060-023-04369-5>.
- [23] Guna A, Stevens TA, Inglis AJ, Replogle JM, Esantsi TK, Muthukumar G, *et al.* MTCH2 is a mitochondrial outer membrane protein insertase. *Science.* 2022; 378: 317–322. <https://doi.org/10.1126/science.add1856>.
- [24] Leibowitz-Amit R, Tsarfaty G, Abargil Y, Yerushalmi GM, Horev J, Tsarfaty I. Mimp, a mitochondrial carrier homologue, inhibits Met-HGF/SF-induced scattering and tumorigenicity by altering Met-HGF/SF signaling pathways. *Cancer Research.* 2006; 66: 8687–8697. <https://doi.org/10.1158/0008-5472.CA.N-05-2294>.
- [25] Peng L, Zhao M, Liu T, Chen J, Gao P, Chen L, *et al.* A stop-gain mutation in GXYLT1 promotes metastasis of colorectal cancer via the MAPK pathway. *Cell Death & Disease.* 2022; 13: 395. <https://doi.org/10.1038/s41419-022-04844-3>.
- [26] Yuan Q, Yang W, Zhang S, Li T, Zuo M, Zhou X, *et al.* Inhibition of mitochondrial carrier homolog 2 (MTCH2) suppresses tumor invasion and enhances sensitivity to temozolomide in malignant glioma. *Molecular Medicine.* 2021; 27: 7. <https://doi.org/10.1186/s10020-020-00261-4>.
- [27] Gao M, Yi J, Zhu J, Minikes AM, Monian P, Thompson CB, *et al.* Role of Mitochondria in Ferroptosis. *Molecular Cell.* 2019; 73: 354–363.e3. <https://doi.org/10.1016/j.molcel.2018.10.042>.
- [28] Duan J, Zhou K, Tang X, Duan J, Zhao L. MicroRNA-34a inhibits cell proliferation and induces cell apoptosis of glioma cells via targeting of Bcl-2. *Molecular Medicine Reports.* 2016; 14: 432–438. <https://doi.org/10.3892/mmr.2016.5255>.
- [29] Camelo-Piragua S, Kesari S. Further understanding of the pathology of glioma: implications for the clinic. *Expert Review of Neurotherapeutics.* 2016; 16: 1055–1065. <https://doi.org/10.1080/14737175.2016.1194755>.
- [30] Jiang X, Liu B, Nie Z, Duan L, Xiong Q, Jin Z, *et al.* The role of m6A modification in the biological functions and diseases.

- Signal Transduction and Targeted Therapy. 2021; 6: 74. <https://doi.org/10.1038/s41392-020-00450-x>.
- [31] Sendinc E, Shi Y. RNA m⁶A methylation across the transcriptome. *Molecular Cell*. 2023; 83: 428–441. <https://doi.org/10.1016/j.molcel.2023.01.006>.
- [32] Zeng C, Huang W, Li Y, Weng H. Roles of METTL3 in cancer: mechanisms and therapeutic targeting. *Journal of Hematology & Oncology*. 2020; 13: 117. <https://doi.org/10.1186/s13045-020-00951-w>.
- [33] Sikorski V, Selberg S, Lalowski M, Karelson M, Kankuri E. The structure and function of YTHDF epitranscriptomic m⁶A readers. *Trends in Pharmacological Sciences*. 2023; 44: 335–353. <https://doi.org/10.1016/j.tips.2023.03.004>.
- [34] Yen YP, Chen JA. The m⁶A epitranscriptome on neural development and degeneration. *Journal of Biomedical Science*. 2021; 28: 40. <https://doi.org/10.1186/s12929-021-00734-6>.
- [35] Li Y, Su R, Deng X, Chen Y, Chen J. FTO in cancer: functions, molecular mechanisms, and therapeutic implications. *Trends in Cancer*. 2022; 8: 598–614. <https://doi.org/10.1016/j.trecan.2022.02.010>.
- [36] Qu J, Yan H, Hou Y, Cao W, Liu Y, Zhang E, *et al.* RNA demethylase ALKBH5 in cancer: from mechanisms to therapeutic potential. *Journal of Hematology & Oncology*. 2022; 15: 8. <https://doi.org/10.1186/s13045-022-01224-4>.
- [37] He L, Li H, Wu A, Peng Y, Shu G, Yin G. Functions of N⁶-methyladenosine and its role in cancer. *Molecular Cancer*. 2019; 18: 176. <https://doi.org/10.1186/s12943-019-1109-9>.
- [38] Zhang C, Huang S, Zhuang H, Ruan S, Zhou Z, Huang K, *et al.* YTHDF2 promotes the liver cancer stem cell phenotype and cancer metastasis by regulating OCT4 expression via m⁶A RNA methylation. *Oncogene*. 2020; 39: 4507–4518. <https://doi.org/10.1038/s41388-020-1303-7>.
- [39] Li W, Hao Y, Zhang X, Xu S, Pang D. Targeting RNA N⁶-methyladenosine modification: a precise weapon in overcoming tumor immune escape. *Molecular Cancer*. 2022; 21: 176. <https://doi.org/10.1186/s12943-022-01652-3>.
- [40] Zhou S, Liu J, Wan A, Zhang Y, Qi X. Epigenetic regulation of diverse cell death modalities in cancer: a focus on pyroptosis, ferroptosis, cuproptosis, and disulfidptosis. *Journal of Hematology & Oncology*. 2024; 17: 22. <https://doi.org/10.1186/s13045-024-01545-6>.
- [41] Xu X, Cui J, Wang H, Ma L, Zhang X, Guo W, *et al.* IGF2BP3 is an essential N⁶-methyladenosine biotarget for suppressing ferroptosis in lung adenocarcinoma cells. *Materials Today Bio*. 2022; 17: 100503. <https://doi.org/10.1016/j.mtbio.2022.100503>.
- [42] Ma L, Chen T, Zhang X, Miao Y, Tian X, Yu K, *et al.* The m⁶A reader YTHDC2 inhibits lung adenocarcinoma tumorigenesis by suppressing SLC7A11-dependent antioxidant function. *Redox Biology*. 2021; 38: 101801. <https://doi.org/10.1016/j.redox.2020.101801>.
- [43] Sun S, Gao T, Pang B, Su X, Guo C, Zhang R, *et al.* RNA binding protein NKAP protects glioblastoma cells from ferroptosis by promoting SLC7A11 mRNA splicing in an m⁶A-dependent manner. *Cell Death & Disease*. 2022; 13: 73. <https://doi.org/10.1038/s41419-022-04524-2>.
- [44] Wang Y, Wang Y, Gu J, Su T, Gu X, Feng Y. The role of RNA m⁶A methylation in lipid metabolism. *Frontiers in Endocrinology*. 2022; 13: 866116. <https://doi.org/10.3389/fendo.2022.866116>.
- [45] Gussyatiner O, Hegi ME. Glioma epigenetics: From subclassification to novel treatment options. *Seminars in Cancer Biology*. 2018; 51: 50–58. <https://doi.org/10.1016/j.semcancer.2017.11.010>.